



LAWRENCE
LIVERMORE
NATIONAL
LABORATORY

Understanding Magnetic Exchange Interactions by the Pressure Dependent Curie Temperature in FeCoNiCuMn High Entropy Alloys

A. E. Perrin, S. K. McCall, M. McElfresh, D. E. Laughlin, M. E. McHenry

July 24, 2019

Journal of Phase Equilibria and Diffusion

Disclaimer

This document was prepared as an account of work sponsored by an agency of the United States government. Neither the United States government nor Lawrence Livermore National Security, LLC, nor any of their employees makes any warranty, expressed or implied, or assumes any legal liability or responsibility for the accuracy, completeness, or usefulness of any information, apparatus, product, or process disclosed, or represents that its use would not infringe privately owned rights. Reference herein to any specific commercial product, process, or service by trade name, trademark, manufacturer, or otherwise does not necessarily constitute or imply its endorsement, recommendation, or favoring by the United States government or Lawrence Livermore National Security, LLC. The views and opinions of authors expressed herein do not necessarily state or reflect those of the United States government or Lawrence Livermore National Security, LLC, and shall not be used for advertising or product endorsement purposes.

Understanding Magnetic Exchange Interactions by the Pressure Dependent Curie Temperature in FeCoNiCuMn High Entropy Alloys

Alice Perrin¹ Scott McCall² Michael McElfresh³ • David E. Laughlin⁴ Michael E. McHenry⁴

1 Massachusetts Institute of Technology, Cambridge, MA 02139

2 Lawrence Livermore National Lab, Livermore, CA 94550

3 Santa Clara University, Santa Clara, CA 95053

4 Carnegie Mellon University, Pittsburgh, PA 15213

Abstract We report the pressure (P) dependent Curie temperature, $T_c(P)$ in a FeCoNiCuMn high entropy alloy (HEA). We analyze $T_c(P)$ in terms of d-orbital contraction to explain changes in magnetic exchange interactions (J_{ex}). Considerations of the d-radius contraction inferred from the composition dependence of T_c in c-Fe-Ni are combined with experimental data for P -dependent lattice constants and magnetic measurements of $T_c(P)$, to calculate contributions of atomic spacing and d-orbital radii to J_{ex} . We show the d-orbital contraction with P captures most of the T_c variation in this alloy.

Keywords calculations _ experimental phase equilibria _ first principles _ multicomponent _ metallic alloys _ material properties _ solid solution

1 Introduction

High entropy alloys (HEAs) are multicomponent systems where configurational entropy is larger than the fusion entropy of most common metals.[1–4] In many HEAs, BCC or FCC phases are entropically stabilized avoiding intermetallic formation to enhance solid solution strengthening.[5] The most frequently studied FCC HEAs are Cantor alloys consisting of equiatomic concentrations of Cr, Mn, Fe, Co, and Ni.[3] The magnetic behavior of the constituent atoms make them natural candidates for magnetic properties. HEAs have been studied for magnetocaloric effect applications primarily based on the hypothesis that the mixing of different atomic species would broaden the magnetic entropy curve and increase the working range of the material while retaining robust mechanical properties,[6–10] though recent work by Law et al. has produced MCE HEAs with a first order magnetostructural transition as well.[11] Magnetic investigations of HEAs have optimized the magnetocaloric effect near room temperature and describe the discrete exchange interactions in the system which act to distribute contributions to the magnetic entropy.[12] Prior work on Cantor-like alloys containing Fe, Co, Ni, Cu and Mn has focused on the study of pairwise exchange bonds between magnetic atoms in the disordered magnetic systems and the dependence of Curie temperature, T_c , on composition and pressure. Curie temperature engineering in metals with direct exchange interactions is based on understanding the T_c dependence on interatomic distances and magnetic d-orbital overlap in predicting the magnetic exchange interactions, J_{ex} , by the Bethe-Slater curve.[13, 14] The Bethe-Slater curve was originally derived semi-empirically considering the Heitler-London theory of the chemical bond in

the context of Heisenberg exchange^[15,16] and the constraints of the Pauli exclusion principle.^[17]

In the context of mean field theory,^[18] Heisenberg exchange interactions^[15] are linearly related to T_c . While the Hartree-Fock equations are on firm theoretical footing, the solution of Schrödinger's equation with Slater determinantal wavefunctions become computationally intractable with increasing number of electrons. Hartree-Fock theory has been supplanted by considerations of a self-consistent field approximation^[19] and the construction of an exchange correlation potential in local spin density functional theory (DFT).^[20-22] There are now many DFT calculations of exchange interactions in transition metal alloys.^[23]

Calculation of exchange interactions in the solid state are treated most correctly in solutions to relativistic Dirac equations.^[24] Exchange integrals in the context of the Heitler-London theory^[25] of the chemical bond were used to construct the Bethe-Slater curve,^[13,14,26] predicting the dependence of J_{ex} on D/d , where D is the transition metal interatomic spacing and d is the spatial extent of magnetic d-orbitals. In practice, exchange is more often discussed semi-empirically using Bethe-Slater curve predictions of 3d transition metal magnetic states. Since the Bethe-Slater curve is rooted in atomic bonding theory it may also be of future interest to view it in the context of universal binding energy ideas.^[27]

The Bethe-Slater curve is often used to highlight changes in exchange with changing atomic spacing, D , for example in Mn-Bi and alloys where increased Mn-Mn distance results in a switch from antiferromagnetic to ferromagnetic exchange.^[29-31] However, consider the change of T_c of the (FCC) disorder γ -Fe-Ni phase with composition (Fig. 1b).^[28,32] Since FCC Fe and Ni have very similar atomic size and lattice constants, the systematic change of T_c is not explained by atomic spacing, D , alone. Both FCC Ni and Fe fall directly on the Bethe-Slater curve (the latter on the left hand, negative antiferromagnetic region of the

curve). Compositions in the binary alloys mimic the shape of the curve through the entirety of the range. We therefore consider a compositional dependence of J_{ex} arising chiefly from d-orbital contraction. The change in T_c for the Fe-Ni alloys depends on band filling causing d-orbital radius contraction with increasing Ni concentration. Thus, we consider atomic spacing, D , and d-orbital extent, d , as distinct variables to assess changes in J_{ex} . Given this evidence for the importance of d-orbital size on assessing change in magnetic exchange, we can assess the magnetic behavior of a system under applied pressure:

$$\begin{aligned} \frac{\partial J(\frac{D}{d})}{\partial P} &= \frac{\partial J(\frac{D}{d})}{\partial(\frac{D}{d})} \frac{\partial(\frac{D}{d})}{\partial P} \\ &= \frac{\partial J}{\partial(\frac{D}{d})} \left(\frac{1}{d} \frac{\partial D}{\partial P} - \frac{D}{d^2} \frac{\partial d}{\partial P} \right) \\ &= \frac{\partial J}{\partial(\frac{D}{d})} \left(\frac{1}{d} \frac{\partial D}{\partial P} - \frac{D}{d} \frac{\partial \ln d}{\partial P} \right) \end{aligned} \quad (\text{Eq 1})$$

The $\frac{\partial J}{\partial(\frac{D}{d})}$ term is from the slope of the Bethe-Slater curve itself. Note that because this leading term reflects the slope of the Bethe-Slater curve, it can be positive or negative depending on where on the curve we start. The term in parentheses can also be positive or negative depending on the relative importance of the pressure dependence of the lattice constant (interatomic spacing) or the extent of the d-orbitals.

2 Experimental Procedure

FeCoNiCuMn HEAs were prepared by first arc melting elemental components multiples times to form a homogeneous ingot. Ingots were melt-spun to quench the alloys and retain a single, disordered FCC phase. Energy dispersive x-ray diffraction measurements were taken in a Paris-Edinburgh cell^[33-35] at the HPCAT 16-BM-B high pressure station at Argonne National Lab's Advanced Photon

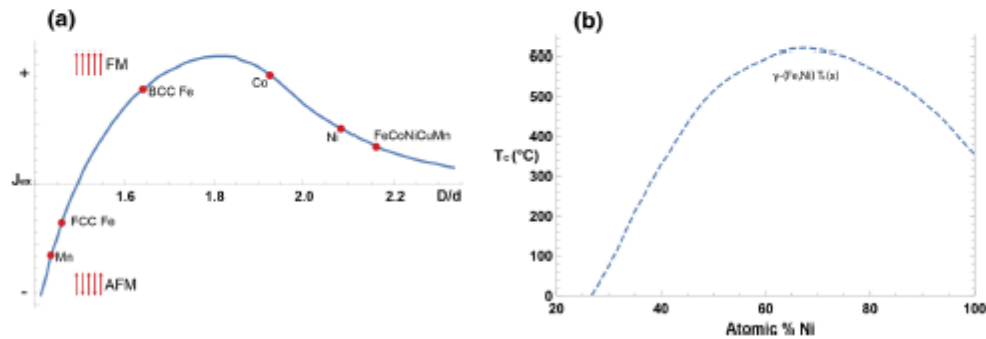


Fig. 1 (a) Bethe Slater Curve, showing the empirical relationship between J_{ex} and D/d . Starting position of FeCoNiCuMn is based on value of T_c and estimated d-orbital size. (b) T_c of the disordered FCC Fe-Ni phase from 20 to 100% Ni, adapted from Swartzendruber^[28].

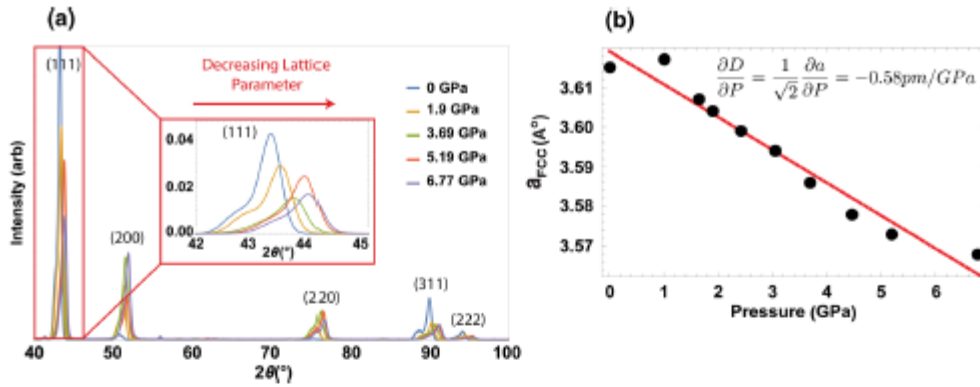


Fig. 2 (a) XRD of FeCoNiCuMn as a function of applied pressure (b) linear relationship between lattice spacing (a) and pressure, with the calculated change in atomic spacing ($D = \frac{a_{fcc}}{\sqrt{2}}$).

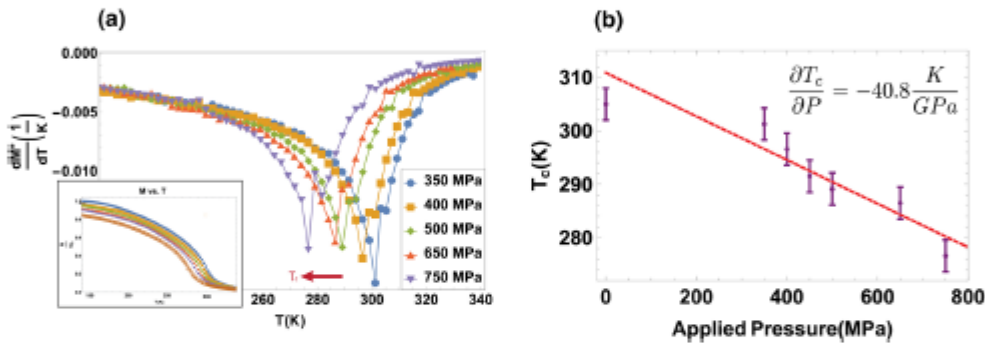


Fig. 3 (a) Curie temperature determined from $\frac{dM}{dT}$ for a series of pressures. The inset shows the $M(T)$ data. (b) The linear T_c vs. P relationship plotted directly.

Source. They were converted to conventional angle-dispersive spectra using Bragg's law. Spectra were taken for several applied pressures up to 6.77 GPa. Magnetic measurements were performed in an M-cell 10 pressure cell fit into a Quantum Design SQUID magnetometer. Each sample was zero field cooled before a heating and cooling magnetization curve were taken at each applied pressure up to 750 MPa. Pressure was determined from the superconducting transition for a Sn manometer.

3 Results and Discussion

To infer the change in the d_{3d} orbital diameter with applied pressure, we first consider experimental data accounting for the remaining terms of Eq 1. The term $\frac{\partial M}{\partial (\frac{D}{a})}$ is taken from the slope of the Bethe Slater curve, which we can parameterize based on expectation values of the diameter of the d-orbitals. D and $\frac{\partial D}{\partial P}$ can be obtained from the high-pressure

x-ray diffraction (XRD) data (Fig. 2a) of FeCoNiCuMn. Peaks were indexed to an FCC structure with an ambient pressure lattice constant of 3.61 Å. Figure 2(b) illustrates the linear pressure dependence of the lattice spacing, a_{fcc} and corresponding atomic spacing, $D = \frac{a_{fcc}}{\sqrt{2}}$. The $\frac{\partial D}{\partial P}$ term in equation 1 is thus -0.58 pm/GPa. The data of Fig. 2(a) allows us to calculate the bulk modulus of the alloy, $K = 175$ GPa. This value is comparable to steels, FCC late transition metals and is considerably larger than softer FCC Mn and Cu; it is also 10% higher than the average bulk modulus of all the elements making up the alloy. This is consistent with the "cocktail effect" noted in the mechanical properties of other HEAs.^[1,2,36,37] This indicates that excellent mechanical properties can be maintained in alloys with sizeable concentrations of elements (Mn, Cu) chosen for their effects in engineering the Curie temperature.

Figure 3(a) illustrates the magnetization, $M(T)$, curves for the FeCoNiCu_{0.95}Mn_{1.05} (19 at.% Cu, 21 at.% Mn) alloy composition described in Kurniawan et al.^[7] The data

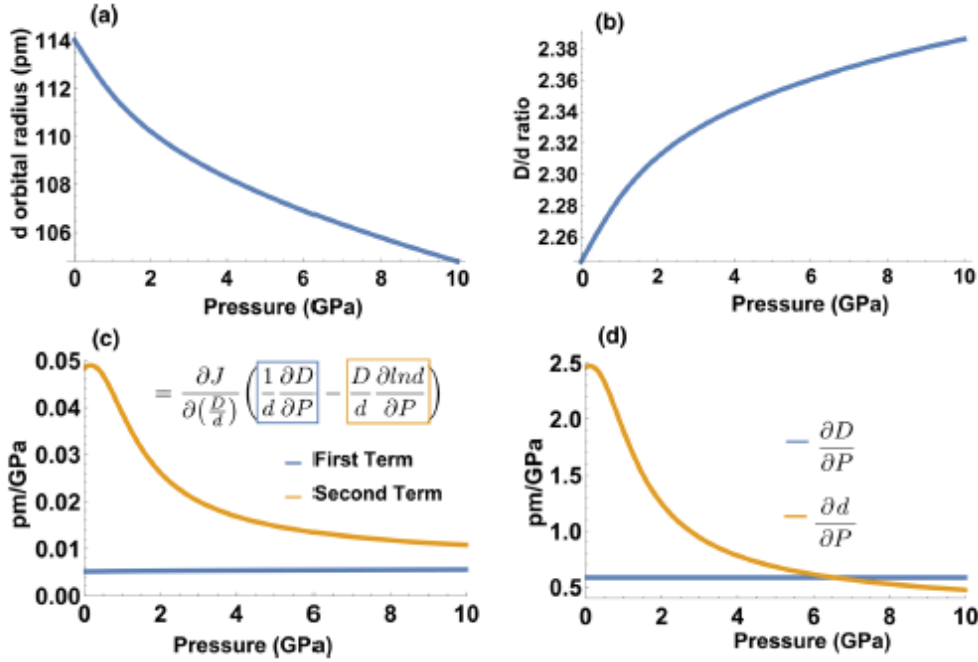


Fig. 4 (a) d orbital diameter versus applied pressure for the FeCoNiCu_{0.95}Mn_{1.05} alloy. (b) D/d ratio with applied pressure, which increases despite both D and d decreasing with pressure. (c) Magnitude of first term and second term from parentheses in equation

1. (d) Magnitude of $\frac{\partial D}{\partial P}$ vs. $\frac{\partial d}{\partial P}$, showing that the change in D becomes greater than the change in d_{3d} around 7 GPa.

shows T_c for this alloy decreases with increasing applied pressure. T_c was estimated from inflection points on the $M(T)$ curves, and calculated more precisely using an Arrott-Noakes equation of state^[38] to ensure an accurate value of the derivative, $\frac{\partial T_c}{\partial P}$, which is equal to -40.8 K/GPa. From the change in T_c with pressure (Fig. 3b) we can estimate the value of $\frac{\partial J}{\partial P}$ using mean field theory:

$$J_{ex} = \frac{3k_B T_c}{2S(S+1)}$$

The mean field value of the spin angular momentum, S , for these alloys was estimated to be $S = 1.5$ based on an average of seven 3d electrons/atom, and comparison with similar alloys and their location on the Slater-Pauling curve. However, it should be noted that the fits are not sensitive to variation of S and thus the exact value used is not significant, as different S values will replicate the same compositional trends where the calculated values are simply scaled upwards. The calculations assume localized d-electrons, but unlike f-electron systems,^[39, Ch. 4] direct exchange is assumed with orbital angular momentum quenched by cubic crys-

tal fields.^[32, Ch. 19] This is consistent with evidence for discrete local pairwise exchange interactions observed in the hyperfine field distributions by Mössbauer spectroscopy.^[6] The FCC structures of these alloys also leads to more localized moments than for BCC structures due to the strong ferromagnetism accompanying a Fermi energy lying in the minority spin d-bands.^[32, Ch. 19] We therefore treat the electrons in these alloys as localized and presume that the chief contribution to the direct exchange interactions is from nearest neighbors. This can be contrasted with BCC FeCo for example where consideration of several nearest neighbor shells is required to capture the exchange.^[23] This experimental data gives us a change in J which can be mapped to the term $\frac{\partial J}{\partial P}$ in Eq 1; combined with the data in

Figure 2 which provides the term $\frac{\partial D}{\partial P}$, we thus have enough data to numerically calculate the $\frac{\partial d_{3d}}{\partial P}$ term in Eq 1 and calculate the average d -orbital size of the FeCoNiCuMn HEA as a function of P (Fig. 4a). The calculations assume the alloy to lie on the righthand side of the Bethe-Slater curve based on its electrons to atom ratio and approximate d -orbital size at $P = 0$, which are close to solid state values calculated by Slater and Mann.^[14, 40]

Our results clearly show the d-orbital contraction, along with d-band filling, and nuclear screening, are important to understanding J_{ex} in alloys. While the Bethe Slater curve is often used to describe the variation of J_{ex} with large atomic spacing variations^[29,30] d-orbital contraction must be considered to precisely account for its variation in disordered alloys with similar interatomic spacings. This is an important consideration in our analysis of T_c (P). Considering changes in atomic spacing (D) alone, we would expect T_c to increase with P in the FeCoNiCuMn HEA given that T_c (P = 0) places it just beyond Ni on the Bethe Slater curve, and decreasing D independent of d would move the point to the left. However, we experimentally observe a decrease in T_c (movement to the right), which we explain by a small decrease in the d-orbital size (a 3.5% decrease at P = 1 GPa). Because the d-orbital decreases in size more rapidly than the atomic spacing, the $\frac{D}{d}$ ratio increases (Fig. 4b).

The relative importance of d-orbital contraction on J_{ex} is evaluated considering the first and second terms in equation 1 separately. The differential in the first term accounts for the change in atomic spacing (D), while the second term depends on the change in d-orbital spatial extent. A direct comparison of the size of each term (Fig. 4c) shows that, particularly at low pressures, the change in d-orbital radius dominates the overall change in exchange J_{ex} . If we directly compare the change in D and d, $(\frac{\partial D}{\partial P})$ vs $(\frac{\partial d}{\partial P})$ (Fig. 4d), the derivative terms intersect at 7 GPa, after which the $\frac{\partial D}{\partial P}$ derivative becomes the larger of the two. However, the non-derivative multipliers for each term scale the influence of each such that the $(\frac{\partial d}{\partial P})$ term always contributes more significantly to changes in J_{ex} . Therefore, it would require enormous, applied pressures to cause a change in sign in J_{ex} . Thus, the inclusion of d-orbital contraction is essential to understand variations in J_{ex} in these HEAs. The initial contraction is postulated to be so large due to the compressibility of the free electrons allowed by their increased density in the FCC interstices of the alloy. This charge redistribution decreases the amount of d-orbital screening between atoms. However, Coulomb repulsion between s and d electrons eventually impedes this compression as orbitals necessarily push closer to the nucleus of neighboring atoms. The crossover at higher applied pressures may provide the driving force for their rotation in a structural or magnetic phase transformation.

There are limits to the conclusions we can draw from these results, primarily due to the distribution of magnetic exchange resulting from the sum of discrete interactions among various magnetic atoms. Mean field theory can only provide an estimate of the exchange energy for this system based on averages. The breadth of the magnetic transitions reflects the fluctuations in exchange interactions about this

average and is a function of the d-orbital extent, also averaged over several atomic species. Additionally, d-orbital behavior is quite complex, and this work alone only contributes experimental grounding and guidance to the larger body of theoretical and computational analysis of d-orbital extent. Nevertheless, this analysis clearly illustrates the relative significance of d-orbital contraction as compared with traditional analysis of interatomic spacings alone in determining J_{ex} .

4 Conclusion

We combine M(T) under pressure data, pressure-varied crystallographic data, and inferences about d-orbital behavior from the disordered γ -phase Fe-Ni T_c to demonstrate the importance of considering atomic spacing and d-orbital radii as separate variables when discussing changes in magnetic exchange energy under pressure. We show that the pressure dependent T_c for a FeCoNiCuMn HEA can be understood to be primarily due to the contraction of d-orbitals.

Acknowledgements The authors acknowledge support from the National Science Foundation (NSF) through Grant DMR-1709247. The authors also acknowledge use of the Data Storage Systems Center at CMU. We thank Alex Leary at NASA Glenn Space Center for measurement assistance. Work at LLNL prepared under Contract DE-AC52-07NA27344 and was supported by the LLNL-LDRD Program under Project No. 20-ER-059.

References

1. J.W. Yeh, Recent Progress in High-Entropy Alloys, *Ann. Chim. Sci. Des Mater.*, 2006, **31**(6), p 633–648. <https://doi.org/10.3166/acsm.31.633-648>
2. J.W. Yeh, Y.L. Chen, S.J. Lin, and S.K. Chen, High-Entropy Alloys—A New Era of Exploitation, *Mater. Sci. Forum*, 2007, **560**, p 1–9.
3. B. Cantor, I.T.H. Chang, P. Knight, and A.J.B. Vincent, Microstructural Development in Equiatomic Multicomponent Alloys, *Mater. Sci. Eng. A*, 2004, **375–377**, p 213–218. <https://doi.org/10.1016/j.msea.2003.10.257>
4. X. Yang, and Y. Zhang, Prediction of High-Entropy Stabilized Solid-Solution in Multi-component Alloys, *Mater. Chem. Phys.*, 2012, **132**(2–3), p 233–238. <https://doi.org/10.1016/j.matchemphys.2011.11.021>
5. Y. Zhang et al., Microstructures and Properties of High-Entropy Alloys, *Prog. Mater. Sci.*, 2014, **61**, p 1–93. <https://doi.org/10.1016/j.pmatsci.2013.10.001>
6. A. Perrin, M. Sorescu, V. Ravi, D.E. Laughlin, and M.E. McHenry, Mössbauer Analysis of Compositional Tuning of Magnetic Exchange Interactions in High Entropy Alloys, *AIP Adv.*, 2019. <https://doi.org/10.1063/1.5079744>
7. M. Kumiawan, A. Perrin, P. Xu, V. Keylin, and M. McHenry, Curie Temperature Engineering in High Entropy Alloys for Magnetocaloric Applications, *Lett IEEE Magn.*, 2016. <https://doi.org/10.1109/LMAG.2016.2592462>

8. A. Perrin, M. Sorescu, M.T. Burton, D.E. Laughlin, and M. McHenry, The Role of Compositional Tuning of the Distributed Exchange on Magnetocaloric Properties of High-Entropy Alloys, *JOM*, 2017, **69**(11), p 2125–2129. <https://doi.org/10.1007/s11837-017-2523-3>
9. M.S. Lucas et al., Thermomagnetic Analysis of FeCoCrNi Alloys: Magnetic Entropy of High-Entropy Alloys, *J. Appl. Phys.*, 2013, **113**(17), p 2011–2014. <https://doi.org/10.1063/1.4798340>
10. B. Fultz, Vibrational Thermodynamics of Materials, *Prog. Mater. Sci.*, 2010, **55**(4), p 247–352. <https://doi.org/10.1016/j.pmatsci.2009.05.002>
11. J.Y. Law et al., MnFeNiGeSi High-Entropy Alloy with Large Magnetocaloric Effect, *J. Alloys Compd.*, 2020, **855**, p 157424. <https://doi.org/10.1016/j.jallcom.2020.157424>
12. K.A. Gallagher, M.A. Willard, V.N. Zabenkin, D.E. Laughlin, and M.E. McHenry, Distributed Exchange Interactions and Temperature Dependent Magnetization in Amorphous Fe₈₈XCoZr₇B₄Cu₁ alloys, *J. Appl. Phys.*, 1999, **85**, p 5130–5132. <https://doi.org/10.1063/1.369100>
13. H. Bethe, and A. Sommerfeld, *Handbuch der Physik* 24. Springer, Berlin, 1933.
14. J.C. Slater, Atomic Shielding Constants, *Phys. Rev.*, 1930, **36**(1), p 57–64. <https://doi.org/10.1103/PhysRev.36.57>
15. W. Heisenberg, Zur Theorie des Ferromagnetismus, *Z. Phys.*, 1928, **49**(9–10), p 619–636. <https://doi.org/10.1007/BF01328601>
16. J.C. Slater, The Theory of Complex Spectra, *Phys. Rev.*, 1929, **34**(10), p 1293–1322. <https://doi.org/10.1103/PhysRev.34.1293>
17. V.W. Pauli, Über den Einfluß der Geschwindigkeitsabhängigkeit der Elektronenmasse auf den Zeemaneffekt, *Z. Physik*, 1924, **31**(1), p 373–385.
18. P. Weiss, The Molecular Field Hypothesis and the Ferromagnetic Property, *J. Phys. Theor. Appl.*, 1907, **6**(1), p 661–690.
19. W. Kohn, and L.J. Sham, Self-Consistent Equations Including Exchange and Correlation Effects, *Phys. Rev.*, 1965, **140**(4A), p A1133–A1138.
20. H. Ebert, D. Ködderitzsch, and J. Minár, Calculating Condensed Matter Properties Using the KKR-Green's Function Method-Recent Developments and Applications, *Rep. Prog. Phys.*, 2011. <https://doi.org/10.1088/0034-4885/74/9/096501>
21. C. Jiang, and B.P. Uberuaga, Efficient Ab Initio Modeling of Random Multicomponent Alloys, *Phys. Rev. Lett.*, 2016, **116**(10), p 1–5. <https://doi.org/10.1103/PhysRevLett.116.105501>
22. P. Hohenberg, and W. Kohn, Inhomogeneous Electron Gas, *Phys. Rev.*, 1964, **136**(3B), p B864–B871. <https://doi.org/10.1007/BF01198136>
23. J.M. MacLaren, T.C. Schulthess, W.H. Butler, R. Sutton, and M. McHenry, Electronic Structure, Exchange Interactions, and Curie Temperature of FeCo, *J. Appl. Phys.*, 1999, **85**, p 4833–4835. <https://doi.org/10.1063/1.370036>
24. P. Dirac, *Principles of Quantum Mechanics (International Series of Monographs on Physics)*, 4th edn. Oxford University Press, Oxford, 1982.
25. V.W. Heitler, and F. London, Wechselwirkung Neutraler Atome und Homopolare Bindung nach der Quantenmechanik, *Z. Phys.*, 1927, **44**, p 455–472.
26. J.C. Slater, Electronic Structure of Alloys, *J. Appl. Phys.*, 1937, **48**, p 385–390.
27. H. Schloesser, J. Ferrante, and J.R. Smith, Global Expression for Representing Cohesive-Energy Curves, *Phys. Rev. B*, 1991, **44**(17), p 9696–9699.
28. L.J. Swartzendruber, V.P. Itkin, and C.B. Alcock, The Fe-Ni (Iron-Nickel) System, *J. Phase Equilibria*, 1991, **12**(3), p 288–311. https://doi.org/10.1007/978-0-387-72264-1_19
29. A. Bruno, and J.P. Lascaray, Nearest and Next Nearest Neighbor Exchange Interaction Between Magnetic Ions in II-VI Semimagnetic Semiconductors, *J. Cryst. Growth*, 1990, **101**(1–4), p 936–939. [https://doi.org/10.1016/0022-0248\(90\)91110-C](https://doi.org/10.1016/0022-0248(90)91110-C)
30. P.J. Webster, and R.S. Tebble, Magnetic and Chemical Order in PdMnAl in Relation to Order in the Heusler Alloys PdMnIn, PdMnSn, and PdMnSb, *J. Appl. Phys.*, 1968, **39**, p 471.
31. B. Cullity, and C. Graham, *Introduction to Magnetic Materials*, 2nd edn. Wiley, Hoboken, 2009.
32. M.E. McHenry, and D.E. Laughlin, *Magnetic Properties of Metals and Alloys*, Vol. 1. Elsevier, Amsterdam, 2014, p 1881
33. A. Yamada et al., High-Pressure x-ray Diffraction Studies on the Structure of Liquid Silicate Using a Paris-Edinburgh Type Large Volume Press, *Rev. Sci. Instrum.*, 2011, **82**, p 1. <https://doi.org/10.1063/1.3514087>
34. G. Shen et al., HPCAT: An Integrated High-Pressure Synchrotron Facility at the Advanced Photon Source, *High Press. Res.*, 2008, **28**(3), p 145–162. <https://doi.org/10.1080/08957950802208571>
35. A.M. Leary et al., The Influence of Pressure on the Phase Stability of Nanocomposite Fe₈₉Zr₇B₄ During Heating from Energy Dispersive x-ray Diffraction, *J. Appl. Phys.*, 2013, **113**(17), p 7–10. <https://doi.org/10.1063/1.4795326>
36. J.W. Yeh et al., Nanostructured High-Entropy Alloys with Multiple Principal Elements: Novel Alloy Design Concepts and Outcomes, *Adv. Eng. Mater.*, 2004, **6**(5), p 299–303. <https://doi.org/10.1002/adem.200300567>
37. S. Ranganathan, Alloyed Pleasures: Multimetallic Cocktails, *Curr. Sci.*, 2003, **85**(10), p 1404–1406.
38. A. Arrott, and J.E. Noakes, Approximate Equation of State for Nickel Near Its Critical Temperature, *Phys. Rev. Lett.*, 1967, **19**(14), p 1–4.
39. R.J. Elliot, Ed., *Magnetic Properties of Rare Earth Metals* Plenum Press, New York, 1972
40. J. B. Mann, *University of California Atomic Structure Calculations Radial Expectation Values: Hydrogen to Lawrencium*, 1968.

This box intentionally left blank